Journal of Photochemistry and Photobiology A: Chemistry 213 (2010) 87–92

Contents lists available at ScienceDirect

Journal of Photochemistry and Photobiology A: Chemistry

journal homepage: www.elsevier.com/locate/jphotochem

Electrolyte effects on photoelectron injection and recombination dynamics in dye-sensitized solar cells

Changneng Zhang, Zhipeng Huo, Yang Huang, Songyuan Dai*, Meng Wang, Yingtong Tang, Yifeng Sui

Key Laboratory of Novel Thin Film Solar Cells, Institute of Plasma Physics, Chinese Academy of Sciences, P.O. Box 1126, Hefei, Anhui 230031, PR China

ARTICLE INFO

Article history:
Received 27 September 2009
Received in revised form 14 April 2010
Accepted 6 May 2010
Available online 25 May 2010

Keywords:
Recombination
Rate constant
Electron injection
Dye-sensitized
Solar cell

ABSTRACT

In this study, the influence of electrolyte on the charge recombination, electron injection efficiency (Φ_{inj}) and performance of dye-sensitized solar cells (DSCs) was investigated. A negative shift in the flatband potential (V_{fb}) of the TiO_2 electrode indicated that 1-methylbenzimidazole (MBI) chemisorbed on the TiO_2 surface and reduced the Li^+ adsorption in the nanostructured electrode. Electrochemical impedance spectra for the DSCs showed that the addition of MBI in the LiI electrolyte could increase the electron lifetime and reduce the rate constant (k_{et}) for I_3^- reduction with electrons in the TiO_2 conduction band. The increase in V_{oc} for solar cells with MBI was mainly attributed to the negative shift in the V_{fb} of the TiO_2 electrode and the decrease of recombination reaction at the dyed TiO_2/electrolyte interface. Analysis of the short-circuit current density (J_{sc}) depended on the light intensity for dye-sensitized solar cells indicated that there was no obvious effect on Φ_{inj} when the LiI concentration was up to 0.7 M in the electrolyte. Due to the negative shift in V_{fb} of the TiO_2 electrode by the addition of MBI in the electrolyte, Φ_{inj} could be reduced to obtain a decreased J_{sc}.

1. Introduction

Dye-sensitized solar cells (DSCs) developed by Grätzel and co-workers have been extensively studied for their high-power conversion efficiency and potential low cost [1–8]. The typical DSC is normally made into sandwich-type photoelectrochemical solar cells between the dyed TiO_2 electrode and the platinized counter electrode, filling with the electrolyte commonly containing the I^-/I_3^- redox couple. Under illumination, photoexcited sensitizers inject electrons into the TiO_2 conduction band. The quantum yield of the photoelectron injection depends on the surface properties of TiO_2 and the nature and concentration of cations in the electrolyte [9]. The injected electrons can transfer to oxidized dye or I_3^- in the electrolyte resulting in the positive shift of the conduction band. Current strategy to improve the performance of DSCs is related to suppressing the charge recombination and increasing the effective electron injection efficiency.

It has been found that cations in the electrolyte could induce a shift in the flatband potential of TiO_2 electrode and affect the rate of electron injection [10,11]. Grätzel reported that the flatband potential equals the Fermi level of the nanostructured TiO_2 electrode, and is sensitive to the contact electrolyte [12]. Redmond and Fitzmaurice investigated cation effects on the flatband potential of the nanostructured TiO_2 electrode by spectroscopic techniques [13]. They found that the increase of cation content in the electrolyte led to a positive shift in the flatband potential through intercalation into the crystal lattice or chemisorption on the surface of the TiO_2 electrode. Meyer and co-workers reported that Li^+ could accelerate the rate of the electron injection from the photoexcited sensitizers into the TiO_2 conduction band, resulting in a larger short-circuit photocurrent and a lower open-circuit voltage [10,11].

Nitrogen-containing heterocycle, such as 1-methylbenzimidazole (MBI) and 4-*t*-butylpyridine (tBP), is widely used due to the effective improvement on the open-circuit voltage of DSCs [14–20]. Schlichthorl et al. found that the addition of tBP in the electrolyte resulted in an increased electron lifetime and a significant upward shift of the conduction band edges [17]. Hagfeldt and co-workers found that the addition of tBP in the electrolyte resulted in a decreased response in the red part of the photocurrent spectrum [18,19]. They ascribed this effect to a negative shift in the TiO_2 conduction band edge. With respect to interface property of the nanostructured TiO_2 electrode in the presence of MBI, we reported the negative shift of the flatband potential resulting in a larger increase in the open-circuit voltage. This result implies that MBI interaction with TiO_2 could suppress Li^+ ions on the surface of nano-TiO_2 electrode [20]. However, there is no detailed study about the influence of the shift in the flatband potential of the nanostructured TiO_2 electrode on the photoelectron injection from the dye to the TiO_2 conduction band and the rate constant for the recombination reaction at the dyed TiO_2/electrolyte interface

* Corresponding author at: Key Laboratory of Novel Thin Film Solar Cells, Institute of Plasma Physics, Chinese Academy of Sciences, P.O. Box 1126, Hefei, Anhui 230031, PR China. Tel.: +86 551 5591377; fax: +86 551 5591377.
E-mail address: sydai@ipp.ac.cn (S. Dai).

1010-6030/$ – see front matter © 2010 Elsevier B.V. All rights reserved.
doi:10.1016/j.jphotochem.2010.05.004

Table 1
Composition and concentration of various electrolytes used in this study.

Electrolyte	DMPII, MBI, LiI
A	0.7 M DMPII
B	0.6 M DMPII, 0.45 M MBI, 0.1 M LiI
C	0.6 M DMPII, 0.1 M LiI
D	0.4 M DMPII, 0.3 M LiI
E	0.7 M LiI
F	0.7 M DMPII, 0.45 M MBI

In this paper, we attempt to study the effect of the negative shift in the flatband potential (V_{fb}) of the nanostructured TiO_2 electrode on the rate constant (k_{et}) for the recombination reaction at the dyed TiO_2/electrolyte interface. And we also study the electron injection efficiency (Φ_{inj}) and photovoltaic performance of DSCs with MBI and Li^+ in the electrolyte.

2. Experimental

2.1. Materials

1-Methylbenzimidazole (MBI) and lithium perchlorate ($LiClO_4$) were obtained from Aldrich. Anhydrous lithium iodide, iodine, and 3-methoxypropionitrile (MePN) were purchased from Fluka. Acetonitrile (MeCN) (chromatographic grade, Haoshen Chemical, Inc., Shanghai, China) was used without further purification. 1,2-Dimethyl-3-propylimidazolium iodide (DMPII) was synthesized as reported previously [15]. Six different electrolytes were employed for DSCs as shown in Table 1.

2.2. DSC assembly

The colloidal TiO_2 nanoparticles were prepared by hydrolysis of titanium tetraisopropoxide as described elsewhere [20]. Nanocrystalline electrodes about 12 μm in thickness were obtained by screen-printing TiO_2 paste on FTO glass (TEC-8, LOF). The TiO_2 film was heated in air for 30 min at 450 °C. The film was immersed in an ethanol solution of 0.5 mM cis-dithiocyanate-N,N′-bis-(4-carboxylate-4-tetrabutylammoniumcarboxylate-2,2′-bipyridine) ruthenium (II) (N719) for 12 h. The platinized counter electrodes were obtained by spraying H_2PtCl_6 solution to FTO glass followed by heating at 410 °C for 20 min. DSCs were fabricated by sealing the counter electrode and the dyed TiO_2 film with thermal adhesive films (Surlyn, Dupont). And the electrolyte was filled from a hole made on the counter electrode, which was later sealed by a cover glass and thermal adhesive films.

2.3. Methods

The photovoltaic performances of DSCs with the active area of 4.0 cm^2 were measured under an illumination of AM 1.5 (100 mW cm^{-2}), which was realized on a solar simulator (Changchun Institute of Optics Fine Mechanics and Physics, Chinese Academy of Science) with a Keithley 2420 source meter.

The flatband potential (V_{fb}) of the nanostructured TiO_2 electrodes was performed by measuring absorbance at 780 nm as a function of the applied potential. For spectroscopic electrochemistry measurement, 4-μm thick TiO_2 film formed the working electrode (2 cm^2 surface area) of a three-electrode photoelectrochemical cell employing a platinum wire counter electrode and an Ag/AgCl reference electrode. Potential control was carried out on a CHI 660A potentiostat, the applied potential being scanned at 5 mV/s. A 780 nm monochromatic light source was obtained from UV–Vis spectrophotometer (TU-1901, PGeneral Instrument Inc., China). For each determination of V_{fb}, a new working electrode and freshly prepared electrolyte solution were used.

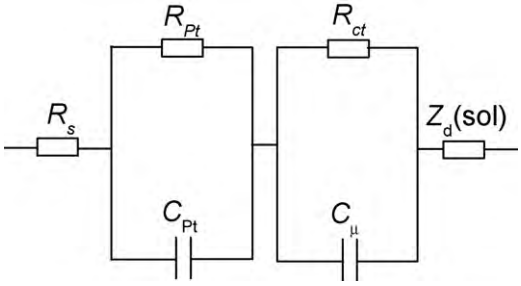

Fig. 1. Equivalent circuit used for the impedance spectra of DSCs. R_s: serial resistance; R_{Pt}: the resistance for charge transfer across the Pt/redox electrolyte interface, C_{Pt}: the chemical capacitance (expressed as a constant phase element) at the Pt/redox electrolyte interface, R_{ct}: the resistance for charge transfer across the TiO_2/redox electrolyte interface, C_μ: the chemical capacitance (expressed as a constant phase element) of the TiO_2 nanoparticles, $Z_{d(sol)}$: the ions diffusion impedance in the electrolyte.

Steady-state voltammograms were recorded on a CHI 660A electrochemical workstation at room temperature in two-electrode mode of DSCs. Impedance measurements were done using an IM6ex electrochemical workstation (Zahner-Elektrick, Germany) in the frequency range of 50 mHz to 1000 kHz at room temperature. The amplitude of the alternative signal was 5 mV. The impedance measurements were carried out in the dark and the obtained spectra were fitted with Z-View software in terms of appropriate equivalent circuit as shown in Fig. 1 [21].

3. Results and discussion

3.1. Effect of additives (1-methylbenzimidazole and LiI) on V_{fb} of the TiO_2 electrode

The role of MBI in the electrolyte in determining V_{fb} of TiO_2 electrode was obtained by spectroelectrochemical techniques, measuring the absorbance at 780 nm as a function of the given potential shown in Fig. 2. The value of V_{fb} determined for 0.5 M $LiClO_4$ in MeCN (−0.74 V vs. Ag/AgCl) was 1.47 V, which was in accordance with the literature [13]. The positive shift in V_{fb} observed at 0.5 M $LiClO_4$ was attributed to the specific adsorption of Li^+ on the TiO_2 electrode. As shown in Fig. 2, the addition of MBI in the electrolyte with 0.5 M $LiClO_4$ produced a value for V_{fb} of −0.98 V, which was 0.24 V more negative than that for $LiClO_4$ in MeCN. This negative shift could be attributed to MBI chemisorption with TiO_2 to reduce the adsorption of Li^+ on the electrode surface.

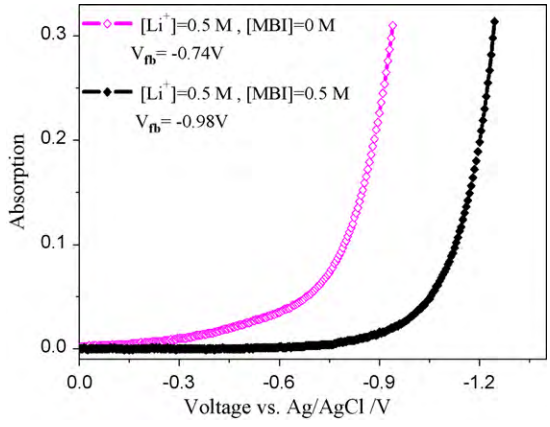

Fig. 2. Absorbance measured at 780 nm as a function of applied potential for a nanostructured TiO_2 electrode in MeCN (0.5 M $LiClO_4$) and with the addition of 0.5 M MBI. The calculated V_{fb} values were obtained by extrapolating the linear portions of these plots, and the applied potential was scanned at 5 mV/s.

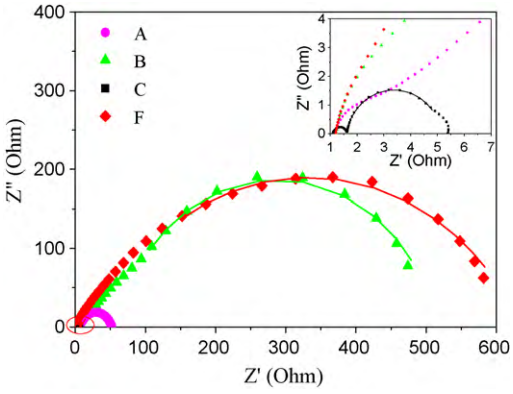

Fig. 3. Nyquist plots of DSCs with electrolytes A–C and F measured at −0.51 V in the dark. The lines show the fitted results. Inset represents enlargement of the area marked with circle.

3.2. Effect of additives on interface recombination in DSCs

Fig. 3 shows the Nyquist plots of DSCs with electrolytes A–C and F measured at forward bias of −0.51 V. The small semicircle in the higher frequencies is due to the counter electrode and could be described by the redox charge transfer resistance (R_{Pt}), and double layer capacitance (C_{Pt}, expressed as constant phase element). The large semicircle at lower frequencies is ascribed to the electron accumulation and recombination processes in the TiO_2 layer, and chemical capacitance (expressed as constant phase element) [21–23]. Fitting the larger semicircle at lower frequency gives the chemical capacitance (C_μ) and the charge transport resistance (R_{ct}) in the EIS experiment. The product of these two quantities gives a time constant, $\tau = R_{ct}C_\mu$, which corresponds to the observed electron lifetime (τ) [23]. When LiI (0.1 M) was added to the 0.7 M DMPII electrolyte (electrolyte A), the chemical capacitance C_μ increased from 2.8 mF to 24.3 mF and the charge transport resistance R_{ct} decreased sharply from 44.2 Ω to 3.5 Ω, yielding the observed τ of 85.1 ms for DSCs with 0.1 M LiI electrolyte (electrolyte C) in comparison with that for DSCs without LiI (electrolyte A), i.e., 123.8 ms. But when MBI (0.45 M) was added to the 0.7 M DMPII electrolyte (electrolyte A), the chemical capacitance C_μ decreased to 0.64 mF and the charge transport resistance R_{ct} increased to 586 Ω, yielding the observed τ of 375 ms for DSCs without LiI in the electrolyte (electrolyte F). It is indicated that a decreased τ for DSCs with 0.1 M LiI electrolyte (electrolyte C) revealed that Li^+ could shift the conduction band of the TiO_2 semiconductor downward and increase the charge recombination at the dyed TiO_2/electrolyte interface. When MBI was introduced to electrolyte C, the chemical capacitance C_μ decreased to 1.3 mF and the electron transport resistance R_{ct} increased sharply to 452.4 Ω, yielding a longer electron lifetime of 588.1 ms for DSCs with MBI in the electrolyte (electrolyte B). It is clearly seen that the addition of MBI in the electrolyte could decrease the recombination reaction with I_3^-, yielding an increased τ for solar cells.

To study the trap distribution in the TiO_2 electrode and the rate constant k_{et} for charge recombination at the dyed TiO_2/electrolyte interface, EIS was measured at different negative applied potentials for DSC with electrolytes A–C. C_μ and R_{ct} have been expressed in the following models [21,24–27].

$$C = C_a \exp\left[\frac{-\alpha eV}{k_B T}\right] + C_b \quad (1)$$

$$R_{ct} = R_{ct}^a \exp\left[\frac{\alpha_t eV}{k_B T}\right] + R_{ct}^b \quad (2)$$

where k_B is the Boltzmann constant, T is the temperature, e is the elementary charge, V is the applied potential, C_a and R_{ct}^a are the pre-exponential factor, C_b is the quasiconstant capacitance at low potentials and R_{ct}^b is the lower charge transfer limit, α is a coefficient describing an exponential distribution of trap states below the conduction band edge ($\alpha < 1$), α_t is the transfer coefficient of the faradic reaction.

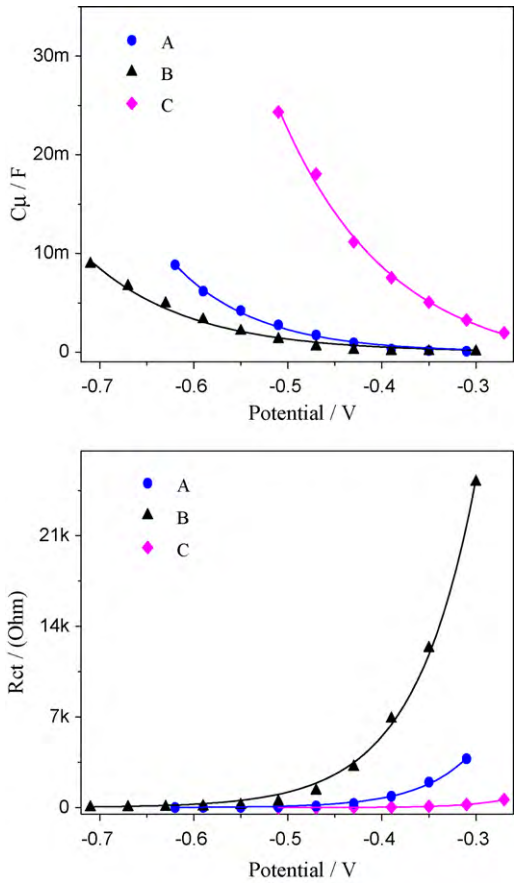

Fig. 4. Results from the impedance data for DSC with electrolytes A–C in the dark at the different applied potentials. (a) Capacitance of DSC with electrolytes A–C. (b) Charge transfer resistance of DSC with electrolytes A–C. The lines indicate the fitted results of C_μ using Eq. (1) and R_{ct} using Eq. (2) as fitting models.

For a (pseudo) first-order recombination reaction with I_3^-, the reaction rate constant k_{et} can be calculated as expressed in Eq. (3) [21].

$$k_{et} = A \cdot \exp\left(\frac{E_a^0 + \alpha_t \cdot F \cdot V}{RT}\right) \quad (3)$$

Here A is the pre-exponential factor, E_a^0 is the activation energy at the potential of 0 V and independent of temperature, and F the Faraday constant. Eq. (3) implies that k_{et} depends on the parameter of α_t and increases with the applied potential at room temperature.

Fig. 4 shows the fitted values of C_μ using Eq. (1) and R_{ct} using Eq. (2) as fitting models. The fit yielded α values from Eq. (1) were 0.29 for DSC without LiI (electrolyte A), 0.28 for DSCs with 0.1 M LiI electrolyte (electrolyte C), and 0.24 for DSC with MBI in the electrolyte (electrolyte B), which was in accordance with the literature [21,26]. This demonstrated that the trap distribution in energy below the TiO_2 conduction band was not affected in the presence of MBI. The fit yielded α_t values from Eq. (2) were 0.48 for DSCs without LiI (electrolyte A), 0.64 for DSCs with 0.1 M LiI electrolyte (electrolyte C), and 0.40 for DSCs with MBI in the electrolyte (electrolyte B). From Eq. (3), we concluded that MBI could decrease k_{et} to retard the recombination reaction in the TiO_2 electrode, which followed the sequence k_{et} (with LiI/MBI) < k_{et} (without LiI) < k_{et} (with LiI).

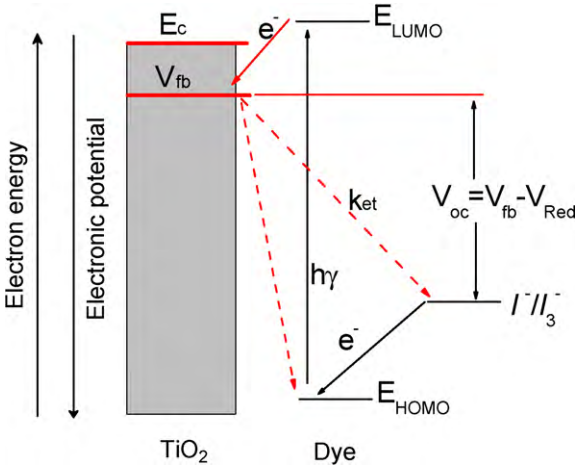

Fig. 5. Energy diagram for DSC with electrolyte containing I^-/I_3^- redox. The energy levels of nano-TiO_2, dye, redox, the photoexcitation process, and the electron injection in the conduction band of nano-TiO_2 are shown in the diagram. The solid arrows indicate electron flowways, while the dashed arrows are the possible recombination pathways with the oxidized sensitizer and with the redox couple.

The predominant recombination in DSCs is expected to be the photoinjected electrons reaction with I_3^- ions, due to the fast regeneration of dye by I^- in the electrolyte. And V_{oc} for DSCs with I^-/I_3^- redox electrolyte is also determined by the following equation [2,28]:

$$V_{oc} = \frac{kT}{e} \ln\left(\frac{I_{inj}}{n_{cb}k_{et}[I_3^-]}\right) \quad (4)$$

where k and T are the Boltzmann constant and absolute temperature, respectively, I_{inj} is the injection electron from dye to semiconductor, n_{cb} the electron concentration at the conduction band edge of semiconductor, and k_{et} the rate constant for the back electron transfer from the conduction band of TiO_2 to I_3^- ions. According to Eq. (4), V_{oc} increases with the decreasing of k_{et}. So MBI chemisorption with TiO_2 to reduce the adsorption of Li^+ could improve the V_{oc} for solar cells.

The increased V_{oc} for DSCs in the presence of MBI compared with that in the absence of MBI may be explained by V_{fb} of the TiO_2 photoelectrode. Under Fermi level pinning, these two parameters are linked by the expression [28,29]

$$V_{oc} = \left|V_{fb} - V_{red}\right| \quad (5)$$

where V_{red} is the standard reduction potential of a redox couple assuming that V_{red} does not vary with the addition of MBI. From the energy diagram of the nanocomposite depicted in Fig. 5 in our cell system, it can be seen that the increased V_{oc} for DSCs with the addition of MBI was due to the negative shift of V_{fb} with MBI chemisorption on TiO_2 photoelectrode to decrease the adsorption of Li^+ on the electrode surface. From Eqs. (4) and (5), we obtain

$$\left|V_{fb} - V_{red}\right| = \frac{kT}{e} \ln\left(\frac{I_{inj}}{n_{cb}k_{et}[I_3^-]}\right) \quad (6)$$

From Eq. (6), it was found that the decrease of the rate constants k_{et} for I_3^- reduction at the TiO_2/electrolyte interface was attributed to the negative shift in V_{fb} of the TiO_2 electrode. It was suggested that the addition of MBI in the electrolyte could rise up the V_{fb} of the TiO_2 electrode and decrease the k_{et} for I_3^- reduction at the TiO_2/electrolyte interface.

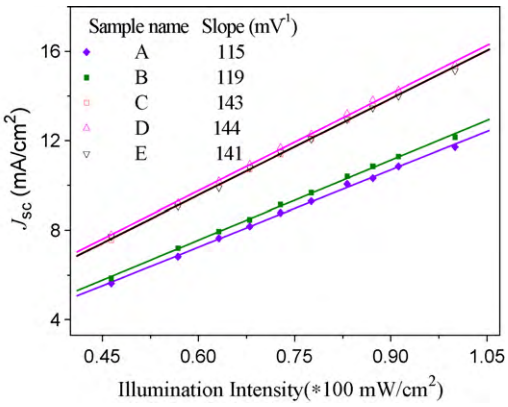

Fig. 6. Short-circuit current J_{sc} as a function of light intensity for DSCs with electrolytes A–E. Inset represents the slopes for electrolytes A–E.

3.3. Effect of additives on photoinjected electrons in DSCs

Fig. 6 shows that the J_{sc} of DSCs with electrolytes A–E varied in direct proportion to the illumination intensity (I) (AM 1.5, 46.4–100 mW cm^{-2}). Because recombination at short circuit is negligible, J_{sc} could be related to the irradiation intensity I by the expression [30].

$$J_{sc} = q\phi AI \quad (7)$$

where q is the electronic charge, A is a constant and depends on the light harvesting efficiency of dye N719 at each wavelength, and ϕ corresponds to the absorbed photon-to-current conversion efficiency at each wavelength (λ) under illumination of solar light.

The slopes in Fig. 6 depended irradiation intensity I was proportional to the ϕ value for DSCs with electrolytes A–E, which indicated the efficiency of electron injection (Φ_{inj}) [30]. The higher slopes for DSCs with electrolytes C–E were indicative of the larger efficiency of electron injection (Φ_{inj}) than that for the electrolyte without LiI, but the increase of LiI concentration from 0.1 M to 0.7 M had little influence on the rate of electron injection. Therefore, in terms of the cell performances, the concentration of LiI should be not more than 0.1 M in the electrolyte. When MBI was added to electrolyte C, the slopes decreased from 143 mV^{-1} to 119 mV^{-1}. The negative shift in the flatband potential of the TiO_2 electrode with MBI would also cause a negative shift in the conduction band edge of TiO_2, which would decrease the energetic overlap between the sensitizer excited state distribution function and the density of semiconductor acceptor states, and explain the decreased slope or the decreased rate of electron injection for DSCs. Our results indicated that the addition of MBI in the electrolyte could decrease the Φ_{inj}, resulting in a decreased J_{sc}.

3.4. Photovoltaic performance of DSCs

Fig. 7 presents the J–V curves of DSCs for the samples with A–C and F under 100 mW cm^{-2} illumination. It can be seen that the solar cells with electrolyte A showed J_{sc} of 11.7 mA cm^{-2}, an open-circuit voltage (V_{oc}) of 0.63 V, fill factor (FF) of 0.63 and energy conversion efficiency (η) of 4.64%. When MBI (0.45 M) was introduced to the 0.7 M DMPII electrolyte (electrolyte A), the V_{oc} and FF of DSCs was obviously improved but J_{sc} became lower. But when LiI (0.1 M) was introduced to the 0.7 M DMPII electrolyte (electrolyte A), the J_{sc} of DSCs was obviously improved but V_{oc} and FF became lower. In our experiments, we found that a significant improved V_{oc} and a slightly enhanced J_{sc} of DSCs with MBI in the electrolyte (electrolyte B) were obtained in comparison with DSCs using the 0.7 M DMPII electrolyte (electrolyte A) (Fig. 7 and Table 2). This indicated that the addition of MBI in the 0.1 M LiI electrolyte was

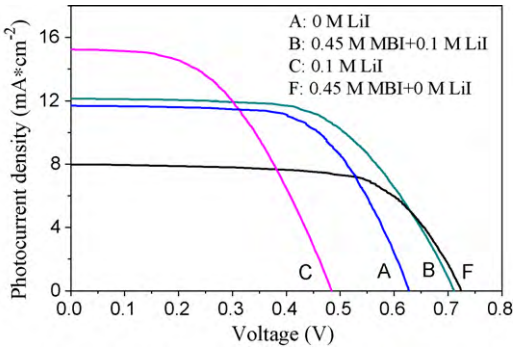

Fig. 7. *J–V* characteristics of the $Ru(dcbpy)_2(SCN)_2$-sensitized solar cells with the electrolytes A–C and F in 100 mW cm^{-2} simulated sunlight. Photovoltaic performances of DSCs are indicated in Table 2.

Table 2
Photovoltaic performance parameters of dye-sensitized solar cells using electrolytes A–C and F.

Electrolyte	J_{sc} (mA cm^{-2})	V_{oc} (V)	*FF*	η (%)
A	11.7	0.63	0.63	4.64
B	12.2	0.71	0.59	5.11
C	15.5	0.51	0.47	3.72
F	8.0	0.72	0.67	3.86

Measured at an irradiation of AM 1.5.

responsible for the enhanced V_{oc} and the improved performance of DSCs.

The J_{sc} for the cells with MBI lower than that for the cells with LiI (Fig. 6) was the result of the decreased Φ_{inj} from the excited dyes. MBI in the electrolyte led to a negative shift in V_{fb} of the TiO_2 conduction band and decreased energetic overlap with the sensitizer excited state donor distribution function, which reduced the electron injection rate so a decreased J_{sc} was obtained. And the addition of MBI in the electrolyte could increase the V_{fb} of the TiO_2 electrode and decrease the k_{et} for I_3^- reduction at the TiO_2/electrolyte interface, resulting in the improvement of V_{oc} and *FF* of the DSCs.

4. Conclusions

In conclusion, the negative shift in V_{fb} of the TiO_2 electrode by the chemisorbed MBI on the electrode surface could decrease the charge recombination reaction with I_3^- and also reduce the electron injection yield from the excited sensitizer. From impedance spectra of the solar cells, it can be concluded that the addition of MBI in the electrolyte could decrease the interfacial faradic reaction on the TiO_2 electrode and did not affect the trap distribution in energy below the conduction band. The improved V_{oc} for solar cells with MBI in the electrolyte resulted from the negative shift in the V_{fb} of the TiO_2 electrode and the reduction of the rate constant (k_{et}) for I_3^- reduction. Analysis of J_{sc} vs. the light intensity for DSCs indicated the higher efficiency of electron injection (Φ_{inj}) for DSCs with various concentrations of LiI in the electrolyte. J_{sc} is slightly reduced due to the decreased Φ_{inj} after adding MBI to the electrolyte.

Acknowledgements

National Basic Research Program of China (Grant No. 2006CB202600), National High Technology Research and Development Program of China (Grant No. 2009AA050603), Foundation of the Chinese Academy of Sciences (Grant No. KGCX2-YW-326), National Natural Science Foundation of China (Grant No. 20703046), and Natural Science Foundation of Anhui Province, China (Grant No. 090414174) are greatly appreciated for financial supports.

References

[1] B. O'Regan, M. Grätzel, A low-cost, high-efficiency solar cell based on dye-sensitized colloidal TiO_2 films, Nature 353 (1991) 737–740.
[2] M.K. Nazeeruddin, A. Kay, I. Rodicio, R.H. Baker, E. Miiller, P. Liska, N. Vlachopoulos, M. Grätzel, Conversion of light to electricity by cis-X_2bis(2,2′-bipyridyl-4,4′-dicarboxylate)ruthenium(II) charge-transfer sensitizers (X = Cl^-, Br^-, I^-, CN^-, and SCN^-) on nanocrystalline TiO_2 electrodes, J. Am. Soc. Chem. 115 (1993) 6382–6390.
[3] M.K. Nazeeruddin, F.D. Angelis, S. Fantacci, A. Selloni, G. Viscardi, P. Liska, S. Ito, B. Takeru, M. Grätzel, Combined experimental and DFT-TDDFT computational study of photoelectrochemical cell ruthenium sensitizers, J. Am. Chem. Soc. 127 (2005) 16835–16847.
[4] Y. Chiba, A. Islam, Y. Watanabe, R. Komiya, N. Koide, L.Y. Han, Dye-sensitized solar cells with conversion efficiency of 11.1%, Jpn. J. Appl. Phys. 45 (2006) L638–L640.
[5] Z.S. Wang, M. Yanagida, K. Sayama, H. Sugihara, Electronic-insulating coating of $CaCO_3$ on TiO_2 electrode in dye-sensitized solar cells: improvement of electron lifetime and efficiency, Chem. Mater. 18 (2006) 2912–2916.
[6] Q. Wang, S. Ito, M. Grätzel, F. Fabregat-Santiago, I. Mora-Sero, J. Bisquert, T. Bessho, H. Imail, Characteristics of high efficiency dye-sensitized solar cells, J. Phys. Chem. B 110 (2006) 25210–25221.
[7] S. Ito, T.N. Murakami, P. Comte, P. Liska, C. Grätzel, M.K. Nazeeruddin, M. Grätzel, Fabrication of thin film dye sensitized solar cells with solar to electric power conversion efficiency over 10%, Thin Solid Films 516 (2008) 4613–4619.
[8] F. Gao, Y. Wang, D. Shi, J. Zhang, M. Wang, X. Jing, R. Humphry-Baker, P. Wang, S.M. Zakeeruddin, M. Grätzel, Enhance the optical absorptivity of nanocrystalline TiO_2 film with high molar extinction coefficient ruthenium sensitizers for high performance dye-sensitized solar cells, J. Am. Chem. Soc. 130 (2008) 10720–10728.
[9] M. Grätzel, J.-E. Moser, Electron Transfer in Chemistry, Wiley-VCH, Weiheim, 2001, 589-644.
[10] D.F. Watson, G.J. Meyer, Cation effects in nanocrystalline solar cells, Coord. Chem. Rev. 248 (2004) 1391–1406.
[11] D.W. Thompson, C.A. Kelly, F. Farzad, G.J. Meyer, Sensitization of nanocrystalline TiO_2 initiated by reductive quenching of molecular excited states, Langmuir 15 (1999) 650–653.
[12] M. Grätzel, Photoelectrochemical cells, Nature 414 (2001) 338–344.
[13] G. Redmond, D. Fitzmaurice, Spectroscopic determination of flat-band potentials for polycrystalline TiO_2 electrodes in nonaqueous solvents, J. Phys. Chem. B 97 (1993) 1426–1430.
[14] H. Kusama, H. Orita, H. Sugihara, TiO_2 band shift by nitrogen-containing heterocycles in dye-sensitized solar cells: a periodic density functional theory study, Langmuir 24 (2008) 4411–4419.
[15] C. Shi, S. Dai, K. Wang, X. Pan, F. Kong, L. Hu, The adsorption of 4-tert-butylpyridine on the nanocrystalline TiO_2 and Raman spectra of dye-sensitized solar cells in situ, Vib. Spectrosc. 39 (2005) 99–105.
[16] H. Kusama, Y. Konishi, H. Sugihara, H. Arakawa, Influence of alkylpyridine additives in electrolyte solution on the performance of dye-sensitized solar cell, Sol. Energy Mater. Sol. Cells 80 (2003) 167–179.
[17] G. Schlichthorl, S.Y. Huang, J. Sprague, A.J. Frank, Band edge movement and recombination kinetics in dye-sensitized nanocrystalline TiO_2 solar cells: a study by intensity modulated photovoltage spectroscopy, J. Phys. Chem. B 101 (1997) 8141–8155.
[18] G. Boschloo, H. Lindstrom, E. Magnusson, A. Holmberg, A. Hagfeldt, Optimization of dye-sensitized solar cells prepared by compression method, J. Photochem. Photobiol. A 148 (2002) 11–15.
[19] G. Boschloo, L. Haggman, A. Hagfeldt, Quantification of the effect of 4-tert-butylpyridine addition to I^-/I_3^- redox electrolytes in dye-sensitized nanostructured TiO_2 solar cells, J. Phys. Chem. B 110 (2006) 13144–13150.
[20] C. Zhang, J. Dai, Z. Huo, X. Pan, L. Hu, F. Kong, Y. Huang, Y. Sui, X. Fang, K. Wang, S. Dai, Influence of 1-methylbenzimidazole interactions with Li^+ and TiO_2 on the performance of dye-sensitized solar cells, Electrochim. Acta 53 (2008) 5503–5508.
[21] C. Zhang, Z. Huo, Y. Huang, L. Guo, Y. Sui, L. Hu, F. Kong, X. Pan, S. Dai, K. Wang, Studies of interfacial recombination in the dyed TiO_2 electrode using Raman spectra and electrochemical techniques, J. Electroanal. Chem. 632 (2009) 133–138.
[22] Z. Huo, S. Dai, C. Zhang, F. Kong, X. Fang, L. Guo, W. Liu, L. Hu, X. Pan, K. Wang, Low molecular mass organogelator based gel electrolyte with effective charge transport property for long-term stable quasi-solid-state dye-sensitized solar cells, J. Phys. Chem. B 112 (2008) 12927–12933.
[23] Q. Wang, J. Moser, M. Grätzel, Electrochemical impedance spectroscopic analysis of dye-sensitized solar cells, J. Phys. Chem. B 109 (2005) 14945–14953.
[24] J.V. Lagemaat, N.-G. Park, A.J. Frank, Influence of electrical potential distribution, charge transport, and recombination on the photopotential and photocurrent conversion efficiency of dye-sensitized nanocrystalline TiO_2 solar cells: a study by electrical impedance and optical modulation techniques, J. Phys. Chem. B 104 (2000) 2044–2052.
[25] J. Bisquert, Chemical capacitance of nanostructured semiconductors: its origin and significance for nanocomposite solar cells, Phys. Chem. Chem. Phys. 5 (2003) 5360–5364.
[26] F. Fabregat-Santiago, I. Mora-Sreo, G. Garcia-Belmonte, J. Bisquert, Cyclic voltammetry studies of nanoporous semiconductors. Capacitive and reactive properties of nanocrystalline TiO_2 electrodes in aqueous electrolyte, J. Phys. Chem. B 107 (2003) 758–768.

[27] Z. Zhang, S.M. Zakeeruddin, B.C. O'Regan, R. Humphry-Baker, M. Grätzel, Influence of 4-guanidinobutyric acid as coadsorbent in reducing recombination in dye-sensitized solar cells, J. Phys. Chem. B 109 (2005) 21818–21824.
[28] H. Kusama, M. Kurashige, H. Arakawa, Influence of nitrogen-containing heterocyclic additives in I^-/I_3^- redox electrolytic solution on the performance of Ru-dye-sensitized nanocrystalline TiO2 solar cell, J. Photochem. Photobiol. A: Chem. 169 (2005) 169–176.
[29] T.S. Kang, K.H. Chun, J.S. Hong, K.J. Kim, Enhanced stability of photocurrent–voltage curves in Ru(II)-dye-sensitized nanocrystalline TiO_2 electrodes with carboxylic acids, J. Electrochem. Soc. 147 (2000) 3049–3053.
[30] M. Yanagida, T. Yamaguchi, M. Kurashige, K. Hara, R. Katoh, H. Sugihara, H. Arakawa, Panchromatic sensitization of nanocrystalline TiO_2 with *cis*-bis(4-carboxy-2-[2′-(4′-carboxypyridyl)]quinoline)bis(thiocyanato-*n*)ruthenium(ii), Inorg. Chem. 42 (2003) 7921–7931.